Int J Adv Manuf Technol (2012) 59:915–928
DOI 10.1007/s00170-011-3562-5

ORIGINAL ARTICLE

Shape error compensation in flexible forming process using overbending surface method

Seong-Chan Heo · Jae-Nam Kim · Woo-Jin Song · Tae-Wan Ku · Beom-Soo Kang

Received: 7 March 2011 / Accepted: 1 August 2011 / Published online: 20 August 2011

Abstract In this article, the design of the flexible forming process considering die shape compensation using an iterative overbending method based on numerical simulation is carried out. In this method, the springback shape obtained from the final step of the first forming simulation is compared with the desired objective shape, and the shape error is calculated as a vector norm with three-dimensional coordinates. The error vector is inversely added to the objective surface to compensate both the upper and lower flexible die configuration. The flexible dies are made up of several punches that make a forming die that is equivalent to a solid die, thus the forming surface shape can be reconfigurable with regard to the compensated die shapes. The flexible die shapes are recalculated, and the punch arrays are adjusted according to the overbent forming surface. These iterative procedures are repeated until the shape error variation converges. In addition, experimental verification is carried out using a 2,000-kN flexible forming apparatus for thick plates. Finally, the configuration of the prototype obtained from the experiment is compared with the numerical simulation results, which have consideration of the springback compensation. Consequently, it is confirmed that the suggested method for compensating the forming error could be used in the design of the flexible forming process for thick-curved plates.

Keywords Flexible forming · Flexible die · Springback compensation · Iterative overbending method · Thick-curved plate forming

S.-C. Heo · J.-N. Kim · B.-S. Kang (✉)
Department of Aerospace Engineering, Pusan National University, Busan 609-735, South Korea
e-mail: bskang@pusan.ac.kr

S.-C. Heo
e-mail: pnuhsc@pusan.ac.kr

J.-N. Kim
e-mail: namgoon07@pusan.ac.kr

W.-J. Song · T.-W. Ku
Industrial Liaison Innovation Center, Pusan National University, Busan 609-735, South Korea

W.-J. Song
e-mail: woodysong@pusan.ac.kr

T.-W. Ku
e-mail: longtw@pusan.ac.kr

1 Introduction

In thin sheet metal-forming processes, iterative modification of the forming process usually would be carried out by numerical and experimental approaches to obtain more accurate products [1, 2]. The main reasons for the configuration errors observed in the metal-forming products are due to roughly designed processes, tool shape errors, unexpected deformation of the blank or billet materials, and the springback effect subsequent to the unloading state [2, 3]. Except for the springback phenomenon, other errors could be mitigated and eliminated by modifying the forming conditions such as the tool shape, forming sequences or steps, forming loads, lubrication, circumferential temperature, and so on. However, the springback is inevitable because it is caused by the mechanical properties of the raw materials that continue elastic recovery [4–6]. Therefore, the springback should be improved by estimating and compensating the elastic behavior of the metallic materials and the products.

Springback phenomenon is also observed even in thick plate-forming process [7–9]. In a flexible forming process for thick-curved plates used for a part of hull structures, the springback is one of the shape error factors besides the discrete flexible die shape itself. The shape accuracy of such plates is important because the plates are to be assembled together through welding for constructing large-hulled structures. In a flexible forming process, these errors could be modified simply through the reconfigurability of the forming apparatus by adjusting the shape of the flexible dies. A reconfigurable die is composed of several forming punches that have a round tip as a forming tool [10–13]. These punches are arranged in a square matrix form in both the upper and lower dies, and they are adjusted according to an objective surface having rather large curvature radii [14, 15]. Owing to reconfigurability, the forming die shapes can be modified in real time in the manufacturing field for compensating the shape errors [16, 17].

In this paper, an iterative modification method for compensating the flexible die shape in the light of springback is proposed by using an iterative overbending surface scheme based on numerical and experimental approaches. In addition, in the present study, the effect of the location of the relative contact point on the forming accuracy was investigated by using the numerical simulation method. In order to verify the feasibility of the springback compensating method, an experiment using a 2,000-kN flexible forming apparatus for thick plates was carried out. The configuration of the deformed thick specimen was compared with the required objective shape. In conclusion, it was confirmed that the proposed iterative overbending surface method was a useful approach for compensating the forming error; thus, it could be used in the modification of the flexible die shape in flexible forming processes for thick-curved plates.

2 Punch height calculation using offset surface method

In a flexible forming process, reconfigurable dies that have several round-tip forming punches are used as the forming tool instead of a one-shot milled solid die set as shown in Fig. 1. The flexible die generates numerous discrete forming surfaces by adjusting its heights according to the objective surface. The calculation of each punch height is based on the prediction of the contact points between the punches and the forming surface. Many researchers have studied the computational scheme using nonuniform rational B-spline and high-precision, triangular-plate bending elements [13]. In the reported studies, the punch heights are determined based on the surface-to-surface contact condition. These approaches involve complicated series of numerical and mathematical formulas. For convenience, a simple method (i.e., the offset surface method) is used in this study for determining the punch heights of the flexible dies.

Usually, the forming punches have a round-tip shape with a uniform radius of curvature as a partial spherical geometry for smoothing the forming surface. Due to the spherical shape of the punch tip, the determination of the punch heights becomes relatively simple. When the partial spherical punches of radius-of-curvature r contact with the forming surface of radius-of-curvature R, the centers of all the punches are to be aligned with a surface that is offset by the punch tip radius r from the forming surface, as shown in Fig. 2. Then, the surface-to-surface contact problem becomes a simpler, point-to-surface problem. In addition, the radii of curvature of the plates used in hull structures are relatively large; thus, the discretized surface that is made up of patches and nodal points from the offset surface can be assumed to be the same as the original curved surface, i.e., the forming surface, as shown in Fig. 3a. Using the discretized rectangular patches, the punch height can be calculated using the above geometrical constraint of the forming punches, namely that the centers of the punches are to be aligned on the offset surface. Among the offset patches, a planar patch that is expressed by Σ_{P} that includes the center of the punch $P(x_{\mathrm{p}}, y_{\mathrm{p}}, z_{\mathrm{p}})$ is investigated to obtain the flexible die shape, as shown in Fig. 3a, because the center point of a punch would be placed on just one patch. When the patches including points of the punches are ascertained, the planar equation of each patch is derived. The equation would be expressed as a function of the coordinates of the nodes $n_i(x_i, y_i, z_i; i = 1 \sim 4)$ that constitute the connectivity of the patches, as shown in Fig. 3b. Thus, the constraint that the center of the punch lies on the patch can be enforced by the following equation:

$$\overrightarrow{N} \cdot \overrightarrow{P} = 0, \qquad (1)$$

where $\overrightarrow{N}$ and $\overrightarrow{P}$ respectively denote the normal vector of the patch and the direction vector from the node, n_1, to the point, $P(x_{\mathrm{p}}, y_{\mathrm{p}}, z_{\mathrm{p}})$, as shown in Fig. 3b. Then, Eq. 1 can be

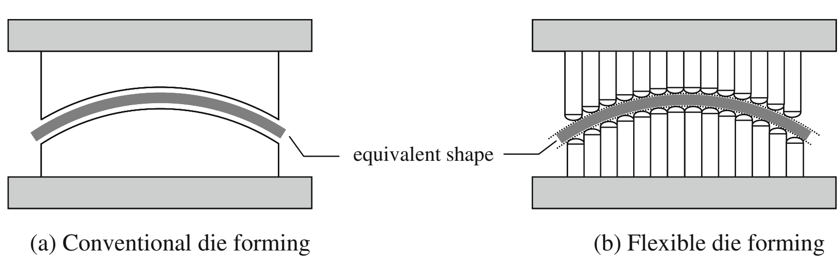

Fig. 1 Schematic view of conventional die forming and flexible forming method. **a** Conventional die forming. **b** Flexible die forming

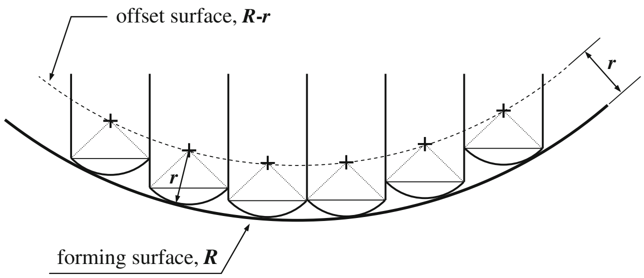

Fig. 2 Geometrical relationship between the centers of round-tip punches and forming surface

expressed by the coordinates of any node, n_i, and of the center point, $P(x_p, y_p, z_p)$, as follows:

$$F(x_p - x_i) + G(y_p - y_i) + H(z_p - z_i) = 0, \tag{2}$$

where $F = (y_2 - y_1)(z_4 - z_1) - (y_4 - y_1)(z_2 - z_1)$,
$G = (x_4 - x_1)(z_2 - z_1) - (x_2 - x_1)(z_4 - z_1)$, and
$H = (x_2 - x_1)(y_4 - y_1) - (x_4 - x_1)(y_2 - y_1)$.

On this occasion, it is assumed that the punch array lies on the x–y plane; thus, the coordinates of x_p and y_p are predetermined values in contrast to z_p, which denotes the required location along the longitudinal direction of the punch to generate an equivalent forming surface. Therefore, Eq. 2 can be expressed in terms of the only unknown, z_p, as follows:

$$z_p = \frac{-F(x_p - x_i) - G(y_p - y_i) + Hz_i}{H}. \tag{3}$$

Equation 3 denotes the expression of the punch height for a punch arrayed at the location of x_p and y_p. Finally, the punch height according to a given forming surface can be calculated by using Eq. 3 for all punches.

For the use of the above method, both the upper and lower offset surfaces made from the forming surface should be prepared. The summation Σ_{pi} over the unit normal direction vectors $\vec{n}_i$ of the adjacent patches for each node

Fig. 3 Determination of punch height using geometrical relationship between the punch centers and discretized offset surface. **a** Determination of patch that includes center of punch. **b** Constraint that center point of punch lies on an offset patch element

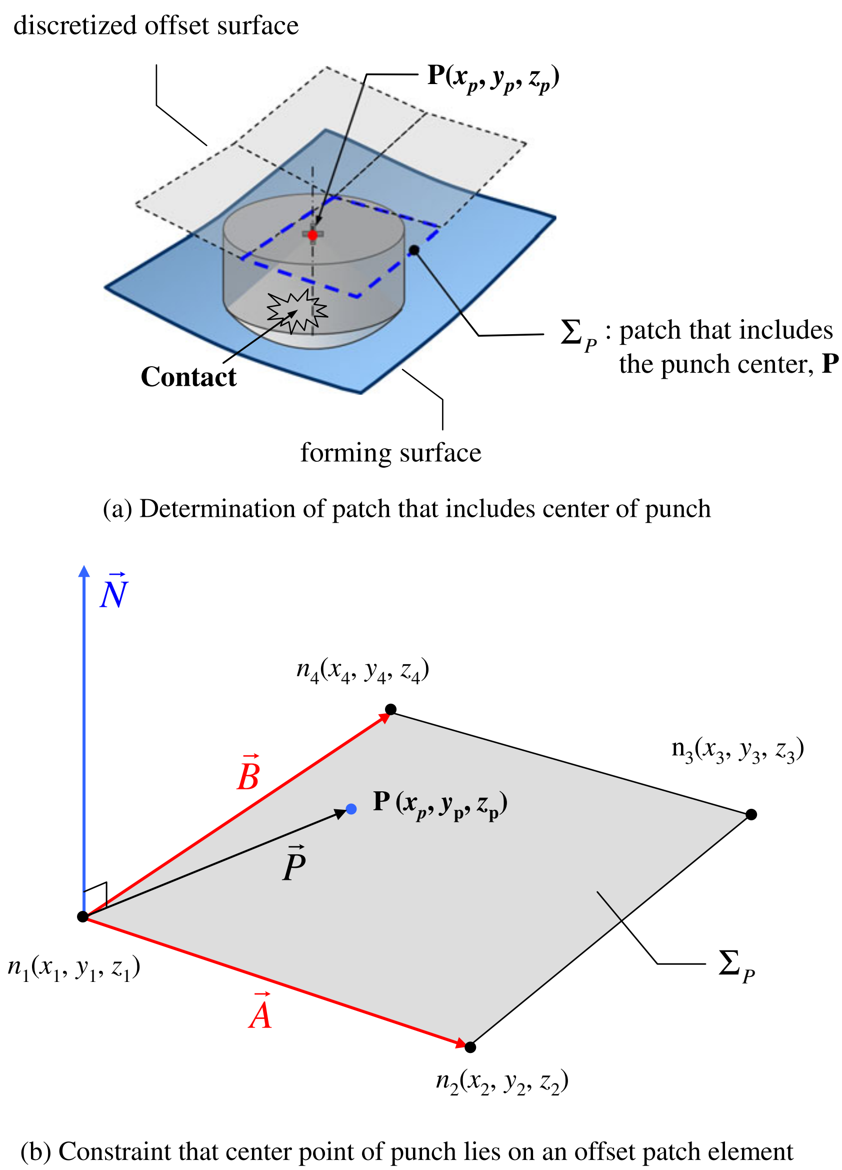

is considered to decide the offset direction, as shown in Fig. 4. As shown in Eq. 4, the vector summation of the adjacent patches, $\sum \vec{n}_i$, is divided by its length to yield the resultant unit direction vector, $\vec{n}_{\text{upper}}$, of the node in the upper direction, which determines the offset direction.

$$\vec{n}_{\text{upper}} = \frac{\left(\vec{n}_1 + \vec{n}_2 + \vec{n}_3 + \vec{n}_4\right)}{\left|\vec{n}_1 + \vec{n}_2 + \vec{n}_3 + \vec{n}_4\right|}. \tag{4}$$

Usually, the objective surface is modeled by referring to the neutral surface of the plate along the thickness direction. Therefore, the offset distance d could be determined by summing up half the thickness of the blank, viz. $\frac{1}{2}b_{\text{t}}$ (i.e., the thickness from the neutral midsurface of the thick plate), the thickness of urethane pads u_{t}, and the punch tip radius r, as shown in Fig. 5. Here, it is assumed that the neutral surface of the objective curved plate remains strain free during the forming process. In addition, for convenience, the variation in the thickness of the plate and in that of the urethane pads during the process is neglected in the alculation of the punch height. Finally, the resultant offset direction vector for the upper side $\vec{\Omega}_{\text{u}}$ is obtained by multiplying the resultant unit direction vector $\vec{n}_{\text{upper}}$ by the offset distance d, i.e., $\vec{\Omega}_{\text{upper}} = d \times \vec{n}_{\text{upper}}$. Similarly, the opposite direction vector for the lower side $\vec{\Omega}_{\text{lower}}$ is also obtained as follows:

$$\vec{\Omega}_{\text{lower}} = -\vec{\Omega}_{\text{upper}}. \tag{5}$$

3 Compensation of springback using iterative overbending method

A flexible die generates various equivalent die shapes with regard to conventional solid dies by adjusting the punch height appropriately according to objective surfaces that have relatively slight curvatures. Figure 6 shows the general procedure of a flexible forming process from the design of the objective surface to the manufacture of the product. Using the objective surface shape, initial curved plate modeling is carried out; further, the model is used to calculate the flexible die shape using the offset surface method. In contrast to the design of a conventional forming process using a solid die, there are two choices in the design of flexible forming processes namely numerical and experimental methods. In an empirical manufacturing procedure based on trial and error, the flexible die has high flexibility and reconfigurability due to its discrete forming surface that comprises forming punches; thus, its die shape can be changed immediately without any additional cost for tool shape modification. This is one of the most valuable characteristics of the flexible forming apparatus; further, due to this flexible characteristic, it is quite appropriate for small-quantity batch production. In the numerical simulation method, a similar procedure as the empirical one would be performed. In the simulations, explicit-to-implicit sequential analysis is conducted using the LS-DYNA solver, which has both the explicit dynamic- and implicit-based codes for the forming and springback simulations, respectively. From the empirical or numerical results, the shape error is examined to determine whether the procedure can progress to production or should revert to die modification. If the shape error does not converge to such a level, the die shape is regenerated. In this study, the numerical method was utilized to design a flexible forming process using finite element analyses and the following iterative overbending method. Although thick plates are used in the flexible forming process for manufacturing hull structures, springback is observed because most of the thick-curved plate parts undergo slight deformation and have large radii of curvature. In addition, springback makes up a considerable portion of the errors observed in the flexible forming processes. Therefore, modification of the die shape for compensating the springback and secondary errors should be undertaken at least more than once—similar to the case of thin sheet metal-forming processes. Also, other errors due to the deformation of the urethane pad and the plate material themselves would be included in the process.

In previous studies, several researchers have sought to minimize and compensate springback by using numerical approaches such as the spring-forward method [18–20] and the displacement adjustment method [21, 22]. In the spring-forward method, the stress state of the blank is calculated, and the external forces are recorded at the end of the forming process. Then, the stresses are inversely imposed using numerical techniques for simulating springback. The displacement adjustment method is used to adjust the die shape until the objective part shape is obtained. The displacement is inversely imposed on the objective surface to make a new die shape. In the method, only the vertical displacement components are considered in the calculation of the displacement.

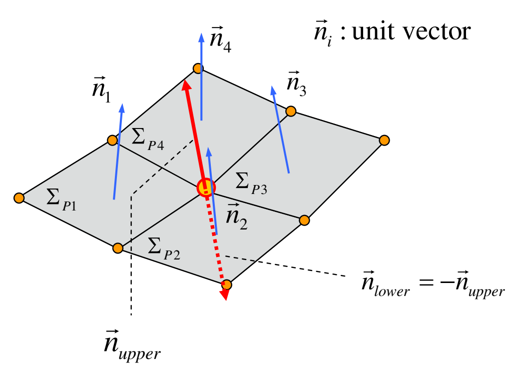

Fig. 4 Determination of nodal offset direction in generating offset surface from discretized patches

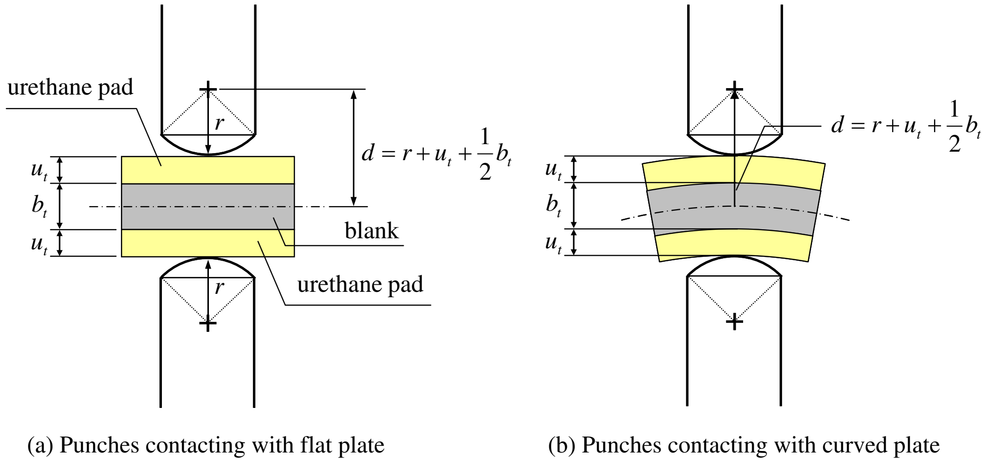

Fig. 5 Equivalence of offset distance from neutral surface of blank to punch center contacting with various flat and deformed blank. **a** Punches contacting with flat plate. **b** Punches contacting with curved plate

In this study, an advanced springback compensation scheme named the overbending surface method that considers the error vector in three-dimensional coordinates is proposed. In this method, the objective shape $\boldsymbol{S}_{\mathrm{obj}}$ is the target shape and is used as a reference configuration for comparing the results regarding deformation. In die shape modification, the shape error vector between the objective surface $\boldsymbol{S}_{\mathrm{obj}}$ and the deformed blank shape $\boldsymbol{S}_{\mathrm{sb}}$ is considered, as shown in Fig. 7a. The error vectors $\vec{E}_i$ at the nodes n_i of the target shape are defined by the direction vectors between the nodes n_i of the objective surface and the nodes $n_i^{\mathrm{sb}}$of the springback surface. A modified shape of the die, $\boldsymbol{S}_{\mathrm{mod}}$, is derived from the vector sum of the direction vectors of the objective surface and the inversed error vectors $-\vec{E}_i$, as shown in Fig. 7b. Similarly, the error vectors in practical three-dimensional problems are derived as shown in Fig. 7c. From the modified forming surface, both the upper and lower surface patches are generated, and the punch heights of both the flexible dies are recalculated for the improved second stage forming process.

4 Application of springback compensation method to flexible forming process

4.1 Flexible forming process using objective surface shape

In this study, a saddle-type curved plate, which is one of the most frequently used types of plate in hull structures, was selected as the application model. The objective surface of the plate with radii of curvature of 1,000 and −1,000 mm and thickness of 10.0 mm is shown in Fig. 8a. As depicted in Fig. 8b, the blank size was 600×600 mm^2, and the number of punches in a flexible die was determined by the punch size. As depicted in Fig. 9a, both the punch width w_{p} and the tip radius r_{p} were 50.0 mm; thus, the number of punches used for the blank was 144 (12×12) for each die according to the blank size. Figure 9b shows the simulation model of the flexible forming process, which includes both the upper and lower flexible dies, urethane pads, and the blank. The punches were assumed to be rigid; thus, only the tips of the punches that contacted with the urethane pads were modeled using shell elements, as shown in Fig. 9b. The blank plate

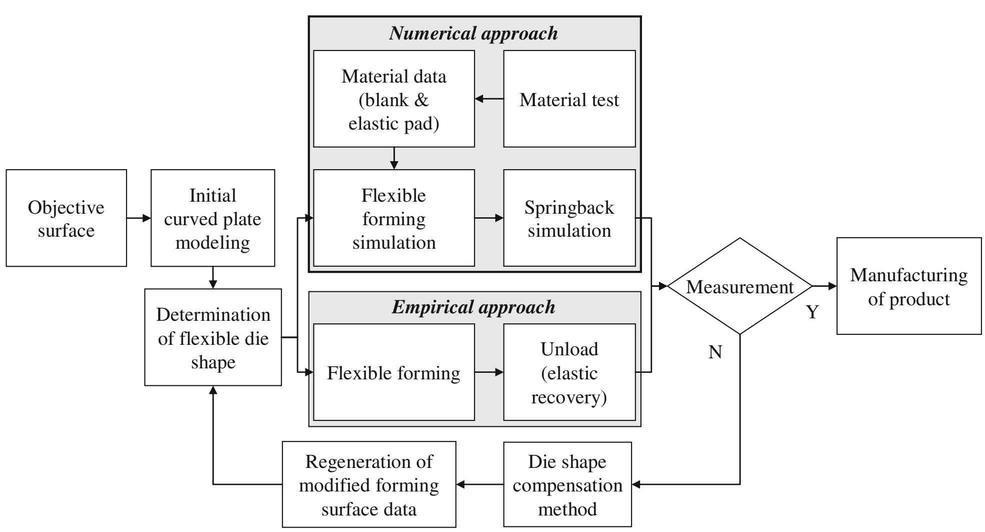

Fig. 6 Design and modification of the flexible forming process using numerical and empirical approaches

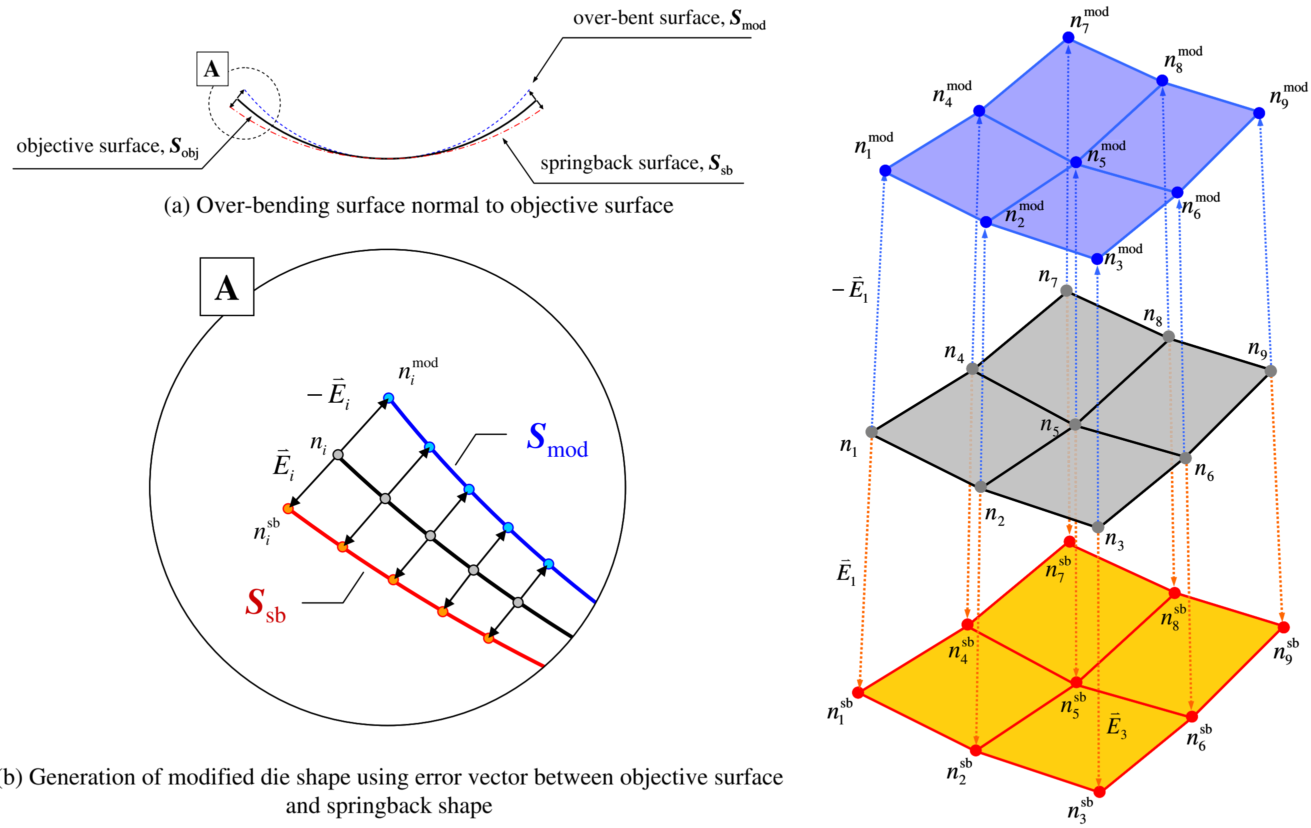

(a) Over-bending surface normal to objective surface

(b) Generation of modified die shape using error vector between objective surface and springback shape

(c) Geometrical relationship of the objective, springback and modified surfaces

Fig. 7 Schematic view of overbending surface method for compensating shape error in flexible forming process. **a** Over-bending surface normal to objective surface. **b** Generation of modified die shape using error vector between objective surface and springback shape. **c** Geometrical relationship of the objective, springback, and modified surfaces

was made up of quadrilayered solid-type elements along the thickness direction. The blank model had 18,605 nodes and 14,400 elements, and the reduced integrated brick element type was used for the elements. In terms of the material properties, the steel plate made of AH32 steel was assumed to follow an elastoplastic material, and the relationship for exponential work-hardening plastic material, $\overline{\sigma} = K\overline{\varepsilon}^n$, was applied for the plastic deformation model with a plastic strength coefficient (K) of 790.5 MPa and a work-hardening exponential (n) of 0.168, which were obtained from the results of a uniaxial tensile test. For the elastic behavior, the Young's modulus E and the Poisson's ratio ν were taken as 210 GPa and 0.29, respectively.

The urethane pads were inserted between the punches and the blank as a practical forming method. An elastic pad had pentalayered solid-type elements along the thickness

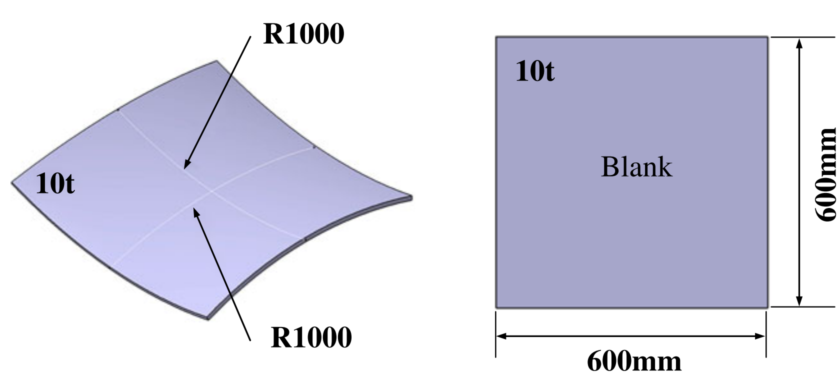

(a) Saddle type curved plate model (b) Dimension of rectangular blank

Fig. 8 Configuration of saddle-type plate model and blank size used in flexible forming process (unit in millimeters). **a** Saddle-type curved plate model. **b** Dimension of rectangular blank

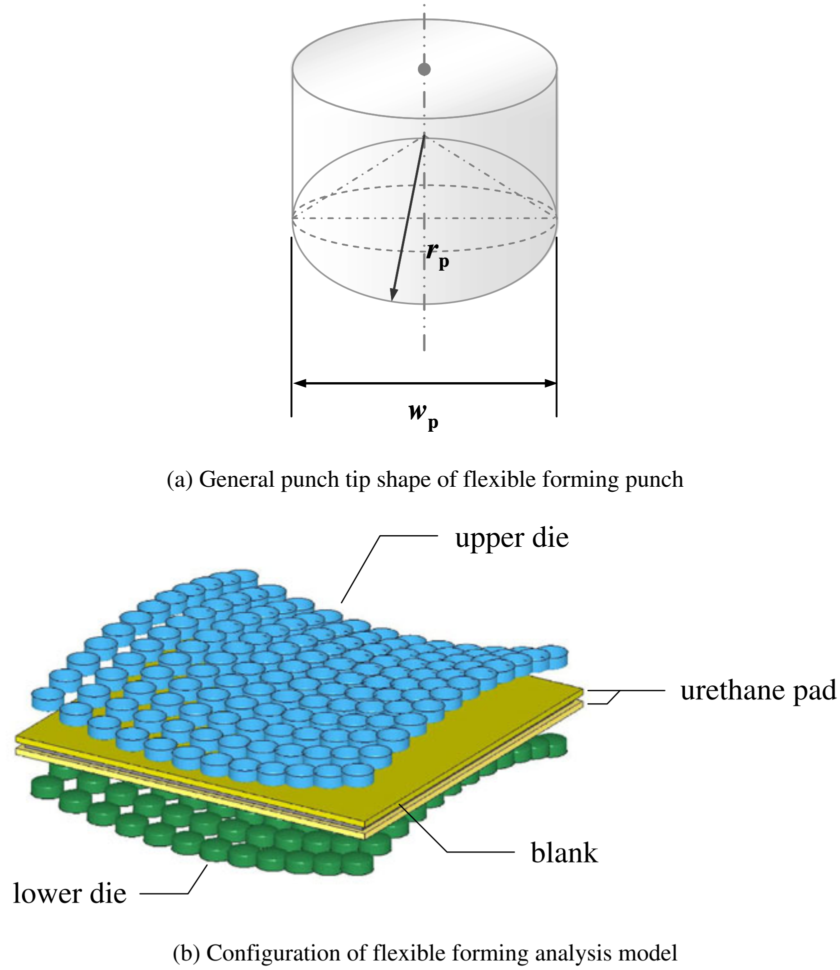

Fig. 9 Punch tip shape and simulation model of flexible forming process. **a** General punch tip shape of flexible forming punch. **b** Configuration of flexible forming analysis model

direction. Each urethane pad model had a fine mesh with 262,086 nodes and 216,320 elements for covering the contacts with the punches that had a relatively small radius of curvature compared with that of the saddle plate. The material properties of the elastic pad are a crucial factor that determines the deformation behaviors in the flexible forming simulation [23]. A nonlinear stress–strain relationship should be considered due to the considerable deformation of urethane pads during the forming process. Usually, urethane with a hardness of shore A90 is used; it exhibits the mechanical behavior of hyperelastic material that can be captured by the Mooney–Rivlin hyperelastic model in the finite element simulation. The Mooney–Rivlin hyperelastic material model with two coefficients is expressed as follows based on the strain energy per unit volume W.

$$W = C_{10}(\overline{I}_1 - 3) + C_{01}(\overline{I}_2 - 3) \quad (6)$$

Here, C_{10} and C_{01} are temperature-dependent material parameters, and $\overline{I}_1$ and $\overline{I}_2$ are the first and second invariants of the deviatoric strain tensor. The nominal stress–strain relationship of the urethane material used in the simulation is shown in Fig. 10. The elastic pads were modeled with a slightly larger area than that of the blank, and their thickness was 10 mm. The friction coefficients between the materials were assumed as 0.1. In the modeling

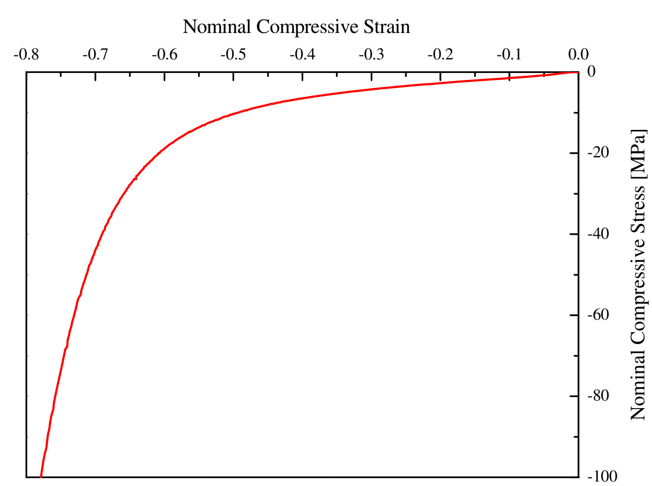

Fig. 10 Nominal compressive stress–strain relationship of urethane pad used in flexible forming analysis

procedure, the calculated punch height data were imported using the ANSYS parametric design language, which is a scripting language that users can use to automate common tasks or even build a model in terms of parameters (variables). Explicit-to-implicit sequential simulations were carried out by using the LS-DYNA explicit solver for the plate-forming analysis; implicit simulations were executed for springback analysis.

Figure 11 shows the configuration of the curved plate and the results obtained from finite element analysis. Figure 11a depicts the configuration of the closed flexible die at the end of the process. The flexible dies are thoroughly closed, contacting with all the punches and urethane pads. The stress and strain distributions of the curved plate at the time are shown in Fig. 11b, c. The maximum stress and the maximum strain of the curved plate were predicted as 418.7 MPa and 0.0234, respectively, at the side edges of the plate. The stress and the strain showed a slightly discrete distribution over the surface due to the discontinuous load that was transferred from the punch array. The simulation results after the springback are shown in the following figures. Figure 11d describes the effective stress distribution of the plate under a maximum stress of 385.1 MPa, and Fig. 11e depicts the strain distribution under a maximum strain of 0.0028. Subsequent to springback, the stress and strain are released from 418.7 to 385.1 MPa and from 0.0234 to 0.0028, respectively. The maximum displacement from the deformed result of the plate after springback is estimated as 4.63 mm.

4.2 Forming accuracy using the iterative overbending method

To investigate the shape error with regard to the objective shape in the neutral surface of the plate, the error distribution of the first simulation result was displayed in a three-dimensional spatial Cartesian coordinates system, as

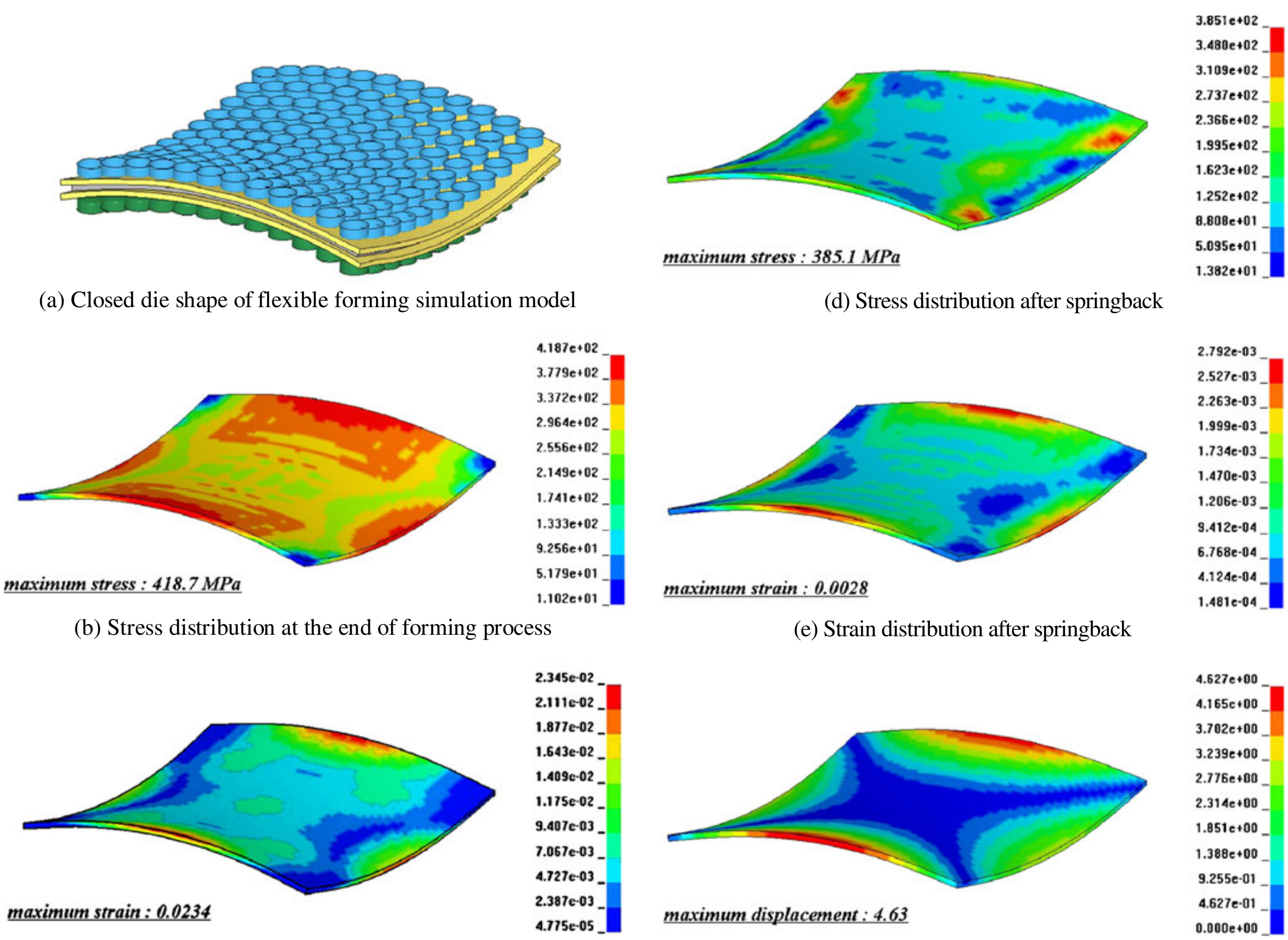

(a) Closed die shape of flexible forming simulation model

(d) Stress distribution after springback

(b) Stress distribution at the end of forming process

(e) Strain distribution after springback

(c) Strain distribution at the end of forming process

(f) Displacement of curved plate after springback

Fig. 11 Finite element analysis results of flexible forming process for saddle-type curved plate. **a** Closed die shape of flexible forming simulation model. **b** Stress distribution at the end of forming process. **c** Strain distribution at the end of forming process. **d** Stress distribution after springback. **e** Strain distribution after springback. **f** Displacement of curved plate after springback

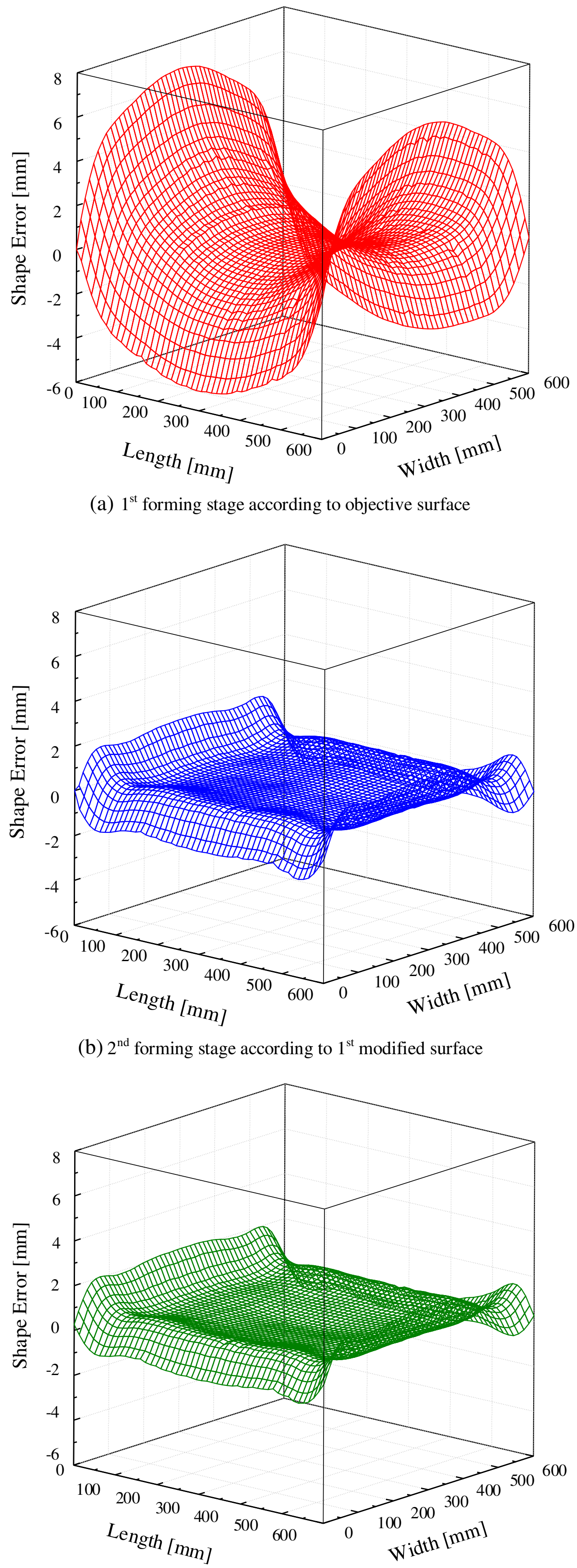

(a) 1st forming stage according to objective surface

(b) 2nd forming stage according to 1st modified surface

(c) 3rd forming stage according to 2nd modified surface

Fig. 12 Shape error distributions of curved plate for various forming stages. **a** First forming stage according to objective surface. **b** Second forming stage according to first modified surface. **c** Third forming stage according to second modified surface

shown in Fig. 12a. From the result, the maximum error was obtained as about 6.5 mm at the edge of the plate. This value was larger than that of the maximum displacement after springback, viz. 4.63 mm, as shown in Fig. 11f. Therefore, it could be inferred that the difference between the springback and error values compared with the objective shape resulted from multiple causes such as complicated compressive deformation of the urethane pads and the discrete die surface, which comprised the forming punches. However, these accumulated errors can be revised by modifying the shape of the flexible die. To compensate the errors in the following second forming stage, the iterative overbending surface method was applied. In this step, the second forming surface, $\boldsymbol{S}_{ob}'$ (i.e., the first modified surface, $\boldsymbol{S}_{mod}$), considering the error vectors, was generated by overbending the springback surface, $\boldsymbol{S}_{sb}$, with the objective surface, $\boldsymbol{S}_{obj}$, as shown in Fig. 7. Similarly, simulations of the second stage flexible forming process were carried out; the error plot of the second forming stage is also displayed in Fig. 12b. As shown in this figure, the distribution of the error in the first stage results with a saddle-type shape definitely improved over the entire area. In contrast to the inner area, the error values steeply increased at the boundary.

To improve the forming accuracy at the boundary, the third stage forming process was additionally carried out by using the third flexible die shapes, $\boldsymbol{S}_{ob}''$ (i.e., the second modified surface, $\boldsymbol{S}_{mod}'$). Figure 12c depicts the error distribution under the third stage forming process. As shown in this figure, the forming error at the boundary did not reduce through the modification of the punch height; the maximum error value was about 2.03 mm. The main reason for these errors at the region was the inherent attribute of a flexible forming process that uses a reconfigurable die set made up of round-tip punches, which

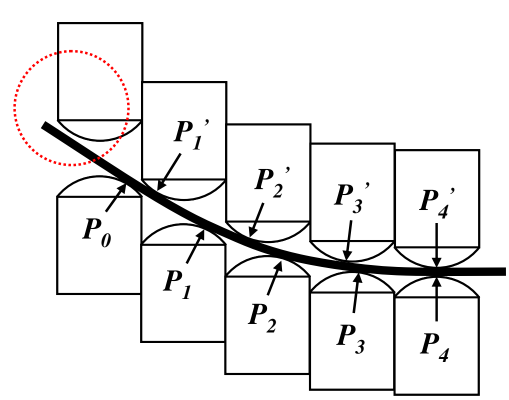

Fig. 13 Cause of forming error due to straight effect in flexible forming process

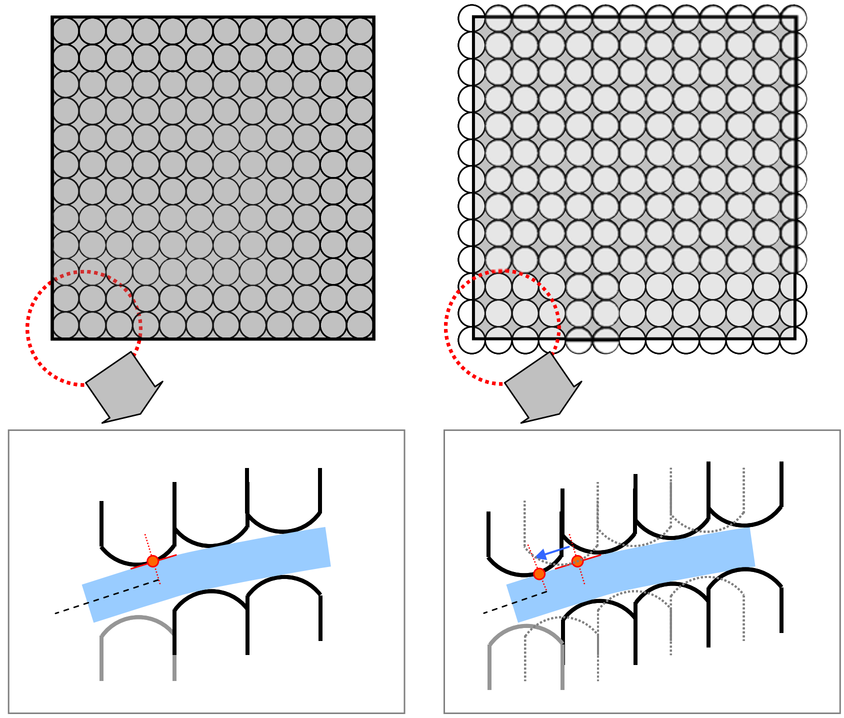
(a) Straight effect zone in array of 12×12 (b) Straight effect zone in array of 13×13

Fig. 14 Improvement of forming accuracy at the boundary by shifting contact point due to relocation of blank with regard to punch array. **a** Straight effect zone in array of 12×12. **b** Straight effect zone in array of 13×13

is called the "straight effect." Basically, flexible forming is based on surface-to-point contact between the blank and punches although elastic pads are inserted to prevent forming failure. Therefore, not only cannot the forming surface at the boundary of the blank be maintained accurately but also the plate shape would remain straight, as shown in Fig. 13. The boundary region of the blank marked with a dotted circle is not fully deformed because the area of accuracy of the forming surface made by the round-tip punches is limited within the contact point P_0 of the outermost punches of the punch array that support the bending force.

4.3 Effect of relative position between blank and punch array on forming accuracy

At the beginning of the design stage, the punch array of dimensions 12×12 was intuitively determined according to the size of the punch with a width of 50 mm and a blank having an area of 600×600 mm^2. On this occasion, however, the inevitable forming error area at the plate boundary was enlarged due to the inappropriate relative position between the punches and the blank. The straight effect zone would be reduced by relocating the blank with regard to the punch array using a 13×13 array. Figure 14a, b shows the improvement in the forming accuracy by the relocation of the blank, which plays the role of shifting the external contact point from the inner area towards the boundary. In this figure, the identical blank size and the curvature shape are used to compare only the forming accuracy and the range of the straight effect zone at the boundary. Actually, as shown in both figures, the punches at the lower left corner would not contribute to the generation of the forming surface due to the straight effect because the curvature shape at the left side of the leftmost contact point on the upper surface of the blank would not be maintained as the objective surface.

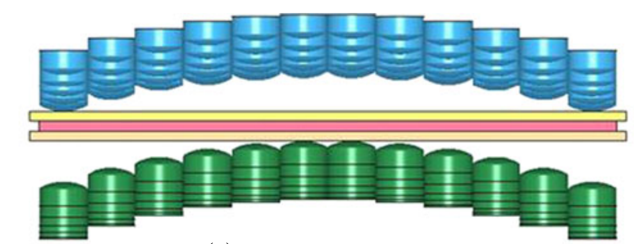
(a) Punch array of 12×12

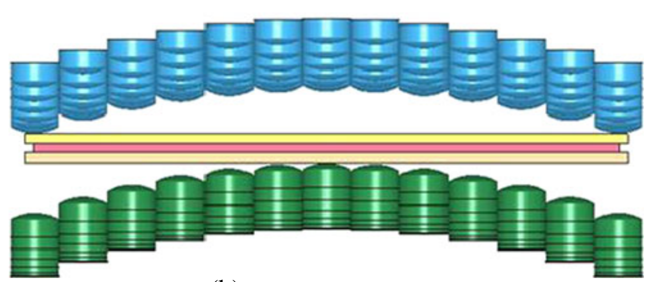
(b) Punch array of 13×13

Fig. 15 Comparison of relative location of blank with regard to two different punch array sizes. **a** Punch array of 12×12. **b** Punch array of 13×13

Therefore, the relative location of the boundary contact point supporting the forming load upon the blank should be moved out towards the boundary as much as possible. By means of shifting, the straight effect zone of the blank can be reduced as shown in Fig. 14b.

According to the relocation approach, the numerical simulation of the flexible forming process and the compensation of the shape error using the iterative overbending surface method were carried out as follows. Figure 15a shows the numerical simulation model having a punch array of 12 × 12; further, the analytic model having a larger forming area than that of the blank due to the use of a punch array of 13 × 13 for modifying the relative position of the blank is shown in Fig. 15b. The modified die model had the same blank and urethane pads as the previous one, and only one row and one column of punches were added. Using this model, the forming analyses were carried out until the second stage of die shape compensation. Similar to the foregoing procedure regarding the simulation results, the error distribution of the second stage result was investigated and compared with the previous results, as depicted in Fig. 16a, b. In these figures, the error plots of both the third stage result using the 12 × 12 punch array and the second stage result using the 13 × 13 array are compared to verify the extent of improvement. The error observed in Fig. 16a would be considered as indicating the extent of improvement in the forming accuracy using the array of 12 × 12. In contrast, the result using the array of 13 × 13 for shifting the contact point to outside of the blank showed considerable improvement in the forming accuracy, as can be seen in Fig. 16b. From the result, the error values were observed to be within about 0.96 mm, which were quite smaller than that of the result obtained from the flexible forming model using the array of 12 × 12, viz. 2.03 mm. Consequently, it was confirmed that the relative position of the blank with regard to the punch array affects the forming accuracy due to the location of the contact point on the

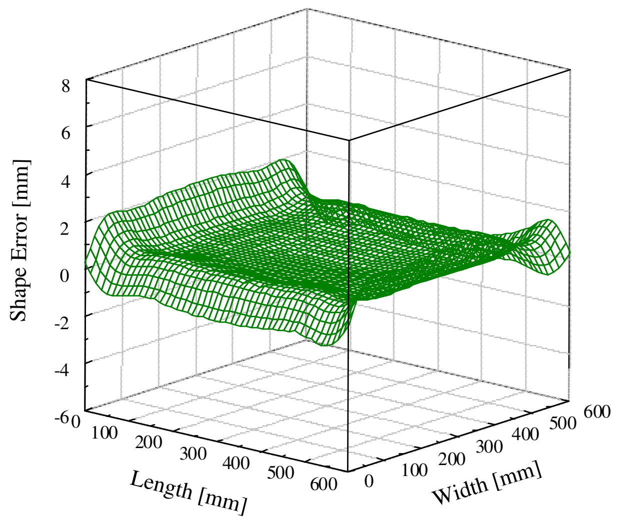

(a) Error distribution of 3rd stage forming procedure using punch array of 12×12

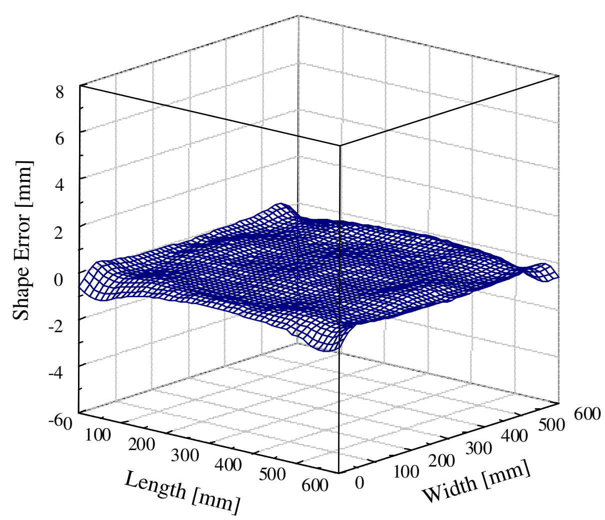

(b) Error distribution of 2nd stage forming procedure punch array of 13×13

Fig. 16 Comparison of relative location of blank with regard to two different punch array sizes. **a** Error distribution of third stage forming procedure using punch array of 12 × 12. **b** Error distribution of second stage forming procedure punch array of 13 × 13

Fig. 17 Flexible forming apparatus with 2,000-kN hydraulic press

blank. Therefore, appropriate positioning of the blank considering the location of the outermost contact points should be determined to obtain better accuracy in the flexible forming process.

5 Experimental investigation

An experiment on curved plate forming for a saddle-type geometry was carried out to confirm the forming accuracy of the modified die shape. Figure 17 depicts the 2,000-kN flexible forming apparatus fabricated for thick plate forming up to a thickness of 25 mm. The forming machine was 4.2 m high, and both the upper and lower flexible die punches were controlled by servo motors. Each flexible die had 192 punches (in a 16×12 array); the length of each punch could be adjusted by adopting a bolt-and-screw assembly structure. The minimum punch length was about 320 mm and could be enlarged up to about 520 mm with a 200-mm stroke range for generating forming surfaces; also,

(a) Flexible die adjusted for saddle-type plate forming

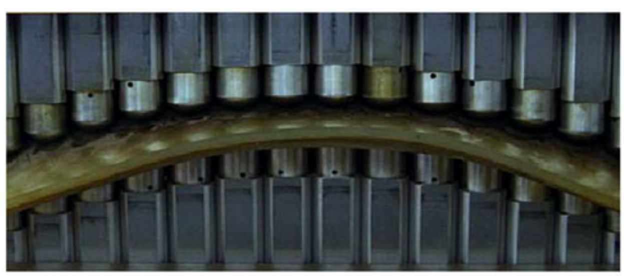

(b) Flexible forming process using urethane pads

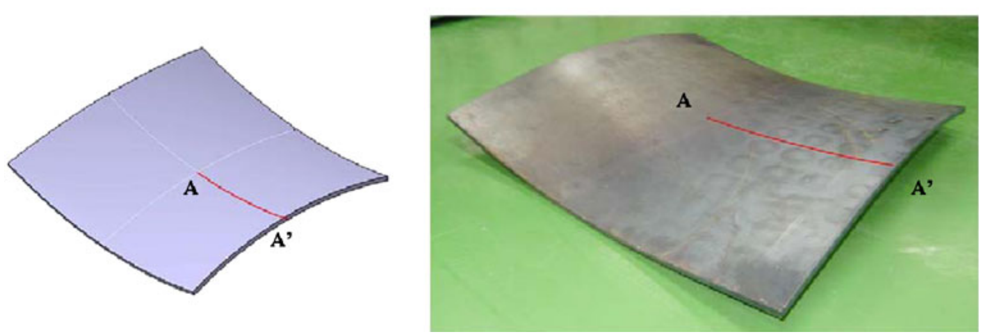

(c) Saddle-type curved plate manufactured by flexible forming process

Fig. 18 Configuration of adjusted punch array for saddle-type curved plate forming process and deformed plate. **a** Flexible die adjusted for saddle-type plate forming. **b** Flexible forming process using urethane pads. **c** Saddle-type curved plate manufactured by flexible forming process the punch tip had a width and radius of 50 mm. An AH32 steel plate with a thickness of 10 mm and a blank size of 600×600 mm^2 was used. Figure 18a shows the flexible die shape that was adjusted to the shape of a saddle. Only the experiment using the 12×12 array was carried out due to the limitation on the punch array size that had only 12 punches along the lengthwise direction, as shown in the figure. Shore A90 urethane pads having 10 mm thickness were used for smoothing the forming surface and preventing defects such as scratches and dimpling caused by contact between both the metallic materials, as shown in Fig. 18b. As a result, the saddle-type curve plate was obtained as seen in Fig. 18c, and it was scanned for comparison with that of the objective surface. Figure 19 depicts a comparison of the major profile of the midsurface along the section A–A′ shown in Fig. 18c with the objective surface and that of the simulations. As shown in this figure, the sectional profiles have good agreement with each other at the center of the curved plate. However, it is confirmed that the profiles have a difference of about 1.9 mm at the boundary due to the straight effect. Nevertheless, it could be concluded that the forming errors originating from various factors in the flexible forming process were considerably reduced by using the modified die shape obtained from the iterative overbending surface method.

6 Conclusion

In this study, a method was proposed for determining the punch height for arbitrary objective forming surfaces. An offset surface scheme considering the geometrical relationship when round-tip punches contact with the forming surface was developed to calculate the punch height. By

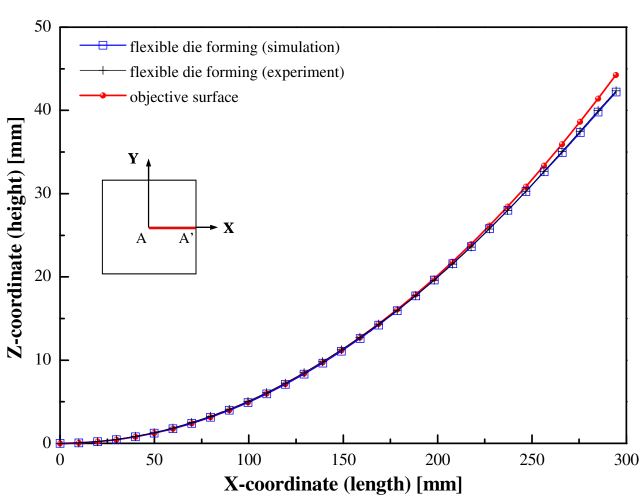

Fig. 19 Sectional profiles according to section *A–A′* of objective surface, simulation, and experimental results

using this method, the surface-to-surface contact problem between the punch tip surfaces and the forming surface could be simplified to a point-to-surface contact problem between the center points of the punches and the forming surface. The vector sum of the adjacent unit normal vectors of each node was used to generate the offset surfaces from the midsurface (i.e., neutral surface) of the objective shape for calculating the punch height. This offset surface generation method was also applied to develop the compensated surface obtained by using the iterative overbending method.

In addition, a compensation method was proposed for the forming error observed in flexible forming processes. An iterative overbending surface method using the numerical simulation method was developed to modify the flexible die shape. To apply the method to a flexible forming process, iterative sequential explicit-to-implicit numerical simulations for the forming and springback processes were carried out with the die shape compensation algorithm. In the method, the shape error vectors were considered to evaluate the forming accuracy and compensate the errors in view of the three-dimensional spatial coordinates. The error vectors were inversely added to the objective surface during the iterative simulation stages. The advantage of the method is that all the factors regarding the shape error such as the deformation of the urethane pads would be compensated by modifying the flexible die shape. In terms of the results, the shape error plots were compared for each step, and it was confirmed that the objective surface would be obtained by using the proposed method. However, it was also observed that the improvement in the forming accuracy by adjusting the punch height was inherently limited due to the straight effect at the boundary of the plate. To minimize the straight effect, the effect of the relative location between the punches and the forming surface on the forming accuracy was investigated. The contact points at the plate boundary were shifted by adding one line of punches in each row and each column of the flexible dies. From the investigation, considerable improvement in the forming accuracy was observed at the boundary of the plate. Therefore, the relative position between the flexible dies and the blank should be considered to minimize the shape error in flexible forming processes.

To verify the feasibility of the methods, an experiment using a 2,000-kN flexible forming apparatus was carried out. It was also noted that the modified shape of the flexible die obtained from the iterative overbending method considerably improved the forming accuracy. Although the effect of the contact points on the blank on the forming accuracy was not confirmed by the experiment due to the limited specification of the forming apparatus, it was confirmed that the relative location also is quite an influential factor in the design of flexible forming process.

Acknowledgments This work was supported by the Korea Science and Engineering Foundation NRL Program grant funded by the Korean government (Ministry of Education, Science Technology—MEST; No. R0A-2008-000-20017-0). Also this work was partially supported by the MEST and Korea Institute for Advancement of Technology through the Human Resource Training Project for Regional Innovation.

References

1. Oral S, Darendeliler H (1997) The optimum die profile for the cylindrical bending of plates. J Mater Process Tech 70:151–155
2. Xue P, Yu TX, Chu E (1999) Theoretical prediction of the springback of metal sheets after a double-curvature forming operation. J Mater Process Tech 89–90:65–71
3. Shu JS, Hung C (1996) Finite element analysis and optimization of springback reduction: the “double-bend” technique. Int J Mach Tool Manufact 36(4):423–434
4. Xue P, Yu TX, Edmund C (2001) An energy approach for predicting springback of metal sheets after double-curvature forming, part I: axisymmetric stamping. Int J Mech Sci 43:1893–1914
5. Meinders T, Burchitz IA, Bonte MHA, Lingbeek RA (2008) Numerical product design: springback prediction compensation and optimization. Int J Mach Tool Manufact 48:499–514
6. Cho JR, Moon SJ, Moon YH, Kang SS (2003) Finite element investigation on springback characteristics in sheet metal U-bending process. J Mater Process Tech 141(1):109–116
7. Borah U, Venugopal S, Nagarajan R, Sivaprasad PV, Venugopal S, Raj B (2008) Estimation of springback in double-curvature forming of plates: experimental evaluation and process modeling. Int J Mech Sci 50(4):704–718
8. Lee JH, Yoon JS, Ryu CH, Kim SH (2007) Springback compensation based on finite element for multi-point forming in shipbuilding. Adv Mater Res 26–28:981–984
9. Li L, Seo YH, Heo SC, Kang BS, Kim J (2010) Numerical simulations on reducing the unloading springback with multi-step multi-point forming technology. Int J Adv Manuf Technol 48:45–61
10. Li MZ, Liu YH, Su SZ, Li GD (1999) Multi-point forming: a flexible manufacturing method for a 3-d surface sheet. J Mater Process Tech 83(1–3):277–280
11. Li MZ, Cai ZY, Sui Z, Yan QG (2002) Multi-point forming technology for sheet metal. J Mater Process Tech 129(1–3): 333–338
12. Li MZ, Cai ZY, Liu CG (2007) Flexible manufacturing of sheet metal parts based on digitized-die. Robot Comput Integr Manuf 23(1):107–115
13. Cai ZY, Li MZ (2002) Multi-point forming of three-dimensional sheet metal and the control of the forming process. Int J Pres Ves Pip 79:289–296
14. Tan FX, Li MZ, Cai ZY, Li XJ (2009) Formability analysis on the process of multi-point forming for titanium alloy retiary sheet. Int J Adv Manuf Technol 41:1059–1065
15. Heo SC, Seo YH, Ku TW, Kang BS (2010) A study on thick plate forming using flexible forming process and its application to a simply curved plate. Int J Adv Manuf Technol 51:103–115
16. Wang SH, Cai ZY, Li MZ (2010) Numerical investigation of the influence of punch element in multi-point stretch forming process. Int J Adv Manuf Technol 49:475–483
17. Liu W, Yang YY, Li MZ (2010) Numerical simulation of multi-point stretch forming and controlling on accuracy of formed workpiece. Int J Adv Manuf Technol 50:61–66
18. Karafillis AP, Boyce MC (2006) Tooling and binder design for sheet metal forming processes compensating spring-back error. Int J Mach Tool Manufact 36:503–526
19. Karafillis AP (1994) Tooling design for three-dimension sheet metal forming using finite element analysis, Dissertation, Massachusetts Institute of Technology
20. Socrate S, Boyce MC (2001) A finite element based die design algorithm for sheet-metal forming on reconfigurable. J Eng Mater Tech 123:489–495
21. Gan W, Wagoner RH, Mao K, Price S, Rasouli F (2004) Practical methods for the design of sheet formed components. J Eng Mater Tech 126:360–367
22. Gan W, Wagoner RH (2004) Die design methods for sheet spring-back. Int J Mech Sci 46:1097–1113
23. Cai ZY, Wang SH, Xu XD, Li MZ (2009) Numerical simulation for the multi-point stretch forming process of sheet metal. J Mater Process Tech 209(1):396–407